Title

Base Excision Repair of N 6 -Deoxyadenosine Adducts of 1,3-Butadiene

Journal

Biochemistry, 55(43)

ISSN

0006-2960

Authors

Wickramaratne, Susith
Banda, Douglas M
Ji, Shaofei
et al.

Publication Date

2016-11-01

DOI

10.1021/acs.biochem.6b00553

Peer reviewed

Published in final edited form as:

Biochemistry. 2016 November 1; 55(43): 6070–6081. doi:10.1021/acs.biochem.6b00553.

Base Excision Repair of N^6-Deoxyadenosine Adducts of 1,3-Butadiene

Susith Wickramaratne[†], **Douglas Banda**[£], **Shaofei Ji**[†], **Amelia H. Manlove**[£], **Bhaskar Malayappan**[†], **Nicole N. Nuñez**[£], **Leona Samson**[δ], **Colin Campbell**[¥], **Sheila David**[£], and **Natalia Tretyakova**[†,*]

[†]Masonic Cancer Center, and the Departments of Chemistry and Medicinal Chemistry University of Minnesota, Minneapolis, MN 55455

[¥]Department of Pharmacology, University of Minnesota, Minneapolis, MN 55455

[δ]Division of Biological Engineering, Massachusetts Institute of Technology, Cambridge, MA 02139

[£]Department of Chemistry, University of California, Davis, CA 95616

Abstract

The important industrial and environmental carcinogen, 1,3-butadiene (BD), forms a range of adenine adducts in DNA, including N^6-(2-hydroxy-3-buten-1-yl)-2′-deoxyadenosine (N^6-HB-dA), 1,N^6-(2-hydroxy-3-hydroxymethylpropan-1,3-diyl)-2′-deoxyadenosine (1,N^6-HMHP-dA), and N^6,N^6-(2,3-dihydroxybutan-1,4-diyl)-2′-deoxyadenosine (N^6,N^6-DHB-dA). If not removed prior to DNA replication, these lesions can contribute to A → T and A → G mutations commonly observed following exposure to BD and its metabolites. In the present study, base excision repair of BD-induced 2′-deoxyadenosine (BD-dA) lesions was investigated. Synthetic DNA duplexes containing site- and stereospecific *S*-N^6-HB-dA, *R,S*-1,N^6-HMHP-dA, and *R,R*-N^6,N^6-DHB-dA adducts were prepared by a post-oligomerization strategy. Incision assays with nuclear extracts from human fibrosarcoma (HT1080) cells have revealed that BD-dA adducts were recognized and cleaved by a BER mechanism, with relative excision efficiency in the order: *S*-N^6-HB-dA > *R,R*-N^6,N^6-DHB-dA > *R,S*-1,N^6-HMHP-dA. Strand cleavage at the adduct site was decreased in the presence of BER inhibitor methoxyamine and by competitor duplexes containing known BER substrates. Similar strand cleavage assays conducted using several eukaryotic DNA glycosylases/lyases [AAG, Mutyh, hNEIL1, and hOGG1] have failed to observe correct incision products at the BD-dA lesion sites, suggesting that a different BER enzyme may be involved in the removal of BD-dA adducts in human cells.

Graphical Abstract

*Corresponding Author: Masonic Cancer Center, University of Minnesota, 2231 6th St. SE - 2-147 CCRB, Minneapolis, MN 55455. Telephone: (612) 626-3432, Fax: (612) 624-3869, trety001@umn.edu.

Supporting information available: characterization of synthetic DNA strands and HPLC-ESI-MS/MS data for excision products.

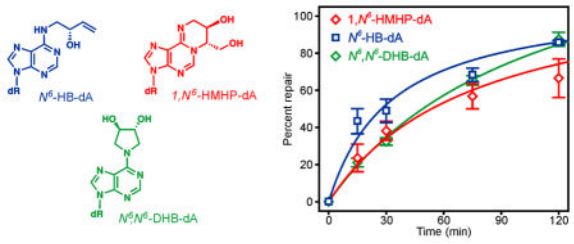

1,3-Butadiene (BD, Scheme 1) is an important industrial and environmental chemical widely used in synthetic rubber and plastic industry and ubiquitously present in automobile exhaust, urban air, and cigarette smoke.[1–3] Based on the results of epidemiological and toxicological studies, BD is classified as a human carcinogen.[4–7] BD is metabolically activated to DNA-reactive epoxides, 3,4-epoxybut-1-ene (EB), 3,4-epoxybutan-1,2-diol (EBD) and 1,2,3,4-diepoxybutane (DEB)[8,9] (Scheme 1). These electrophilic species, if not detoxified, can react with DNA to form a range of nucleobase lesions including DNA monoadducts,[10–12] exocyclic lesions,[13,14] DNA-DNA cross-links,[15–18] and DNA-protein cross-links.[19,20]

The bulk of BD-induced adducts are formed at the *N7*-guanine position of DNA: this adducts (e.g. *N7*- (2-hydroxy-3-buten-1-yl)-2′-deoxyguanosine) are hydrolytically labile and are removed by spontaneous depurination.[21] The less abundant adenine lesions (~ 10% of the total) are of special interest because of their hydrolytic stability and the tendency of BD and its metabolites to cause A → T and A → G mutations.[9,22–24] Multiple BD-dA adducts have been identified, including N^6-(2-hydroxy-3-buten-1-yl)-2′-deoxyadenosine (N^6-HB-dA), 1,N^6-(2-hydroxy-3-hydroxymethylpropan-1,3-diyl)-2′-deoxyadenosine (1,N^6-HMHP-dA) and N^6,N^6-(2,3-dihydroxybutan-1,4-diyl)-2′-deoxyadenosine (N^6,N^6-DHB-dA) (Scheme 1).[10,12,13] N^6-HB-dA is formed upon single alkylation of the N^6 position of adenine in DNA by 3,4-epoxy-1-butene,[12] while 1,N^6-HMHP-dA and N^6,N^6-DHB-dA are induced by *bis*-alkylation of N^6-adenine by 1,2,3,4-diepoxybutane (Scheme 1).[13]

Our recent studies conducted with DNA templates containing site- and stereospecific BD-DNA adducts have revealed that in primer extension experiments, (*S*)-N^6-HB-dA adducts were readily bypassed by human polymerases β, η, and κ in an error-free fashion, while (*R,S*)-1,N^6-HMHP-dA exocycles completely blocked DNA replication by human polymerase β.[25,26] Human translesion synthesis (TLS) polymerases η and κ were able to bypass (*R,S*)-1,N^6-HMHP-dA, introducing T, A, or G opposite the lesion and inducing frameshift mutations.[25,26] Polymerase bypass of (*R,R*)-N^6,N^6-DHB-dA by TLS polymerases was extremely inefficient, with all four nucleotides inserted opposite the modified base with similar frequencies.[25] These results suggest that 1,N^6-HMHP-dA and N^6,N^6-DHB-dA are capable of inducing mutations in the absence of repair. Therefore, an understanding of the cellular repair of BD-dA adducts will aid in defining the biological consequences of these lesions.

In the present study, we investigated the ability of nuclear protein extracts from human fibroblasts and recombinant base excision repair (BER) enzymes to recognize and cleave site- and stereo-specific BD-dA adducts: *S*-N^6-(2-hydroxy-3-buten-1-yl)-2′-deoxyadenosine (*S*-N^6-HB-dA), *R,S*-1,N^6-(2-hydroxy-3-hydroxymethylpropan-1,3-diyl)-2′-deoxyadenosine

(*R,S*-1,N^6-HMHP-dA) and *R,R*-N^6,N^6-(2,3-dihydroxybutan-1,4-diyl)- 2′-deoxyadenosine (*R,R*-N^6,N^6-DHB-dA) (Scheme 2). We found that all three adducts can be excised by nuclear protein extracts from human cells, with efficiency comparable to that of other known BER substrates (1,N^6-ethenoadenine, guanidinohydantoin and 5-fluorouracil, Scheme 2). However, recombinant glycosylases examined [mouse Mutyh, human AAG, hNEIL1 and hOGG1] failed to produce correct excision products, suggesting that a different BER enzyme or accessory protein factors are required for BD-dA adduct repair in cells.

Experimental Procedures

Materials

Protected 2′-deoxyribonucleoside-3′-phosphoramidites (PAC-dA-CE, Ac-dC-CE, *p*-*i*Pr-PAC-dG-CE, dT-CE, 8-oxo-dG-CE, 1,N^6-etheno-dA-CE, 5-fluoro-dC-CE) Ac-dC-CPG ABI and *p*-*i*Pr-PAC-dG-CPG ABI columns, and all other reagents necessary for automated DNA synthesis were purchased from Glen Research (Sterling, VA). 5′-*O*-(4,4′-dimethoxytrityl)-3′-*O*-(2-cyanoethyl)-*N,N*-diisopropyl-phosphoramidite of 6-chloropurine-2′-deoxyriboside was purchased from ChemGenes Corp. (Wilmington, MA). Synthetic DNA oligodeoxynucleotides were prepared by solid phase synthesis using an ABI 394 DNA synthesizer (Applied Biosystems, CA). DNA oligodeoxynucleotides containing 8-oxo-dG and thymine glycol were purchased from Integrated DNA Technologies (Coralville, IA) and Sigma Aldrich (St. Louis, MO), respectively. T4 polynucleotide kinase (T4-PNK) was obtained from New England Biolabs (Beverly, MA), while T4 DNA ligase was procured from Roche (Basel, Switzerland). γ-^{32}P ATP was purchased from Perkin-Elmer Life Sciences (Boston, MA). 40% 19:1 acrylamide/bis solution and micro bio-spin 6 columns were purchased from Bio-Rad (Hercules, CA). Illustra NAP-5 desalting columns and Sep-Pak C18 SPE cartridges were obtained from GE Healthcare (Pittsburg, PA) and Waters (Milford, MA), respectively. All other chemicals and solvents were purchased from Sigma-Aldrich (Milwaukee, WI) and used without further purification.

Cell culture—Chinese hamster lung fibroblast cell lines V79 (GM16136) were obtained from the Coriell Institute for Medical Research (Camden NJ). Cells were grown to 80–90% confluence on tissue culture dishes in Ham's F-12 modified essential Eagle's media (Life Technologies, Grand Island, NY, USA) supplemented with 9% fetal bovine serum. Cells were maintained in a humidified atmosphere of 5% carbon dioxide, 95% air, at 37 °C.

1,N^6-HMHP-dA adduct persistence in genomic DNA detected by isotope dilution HPLC-ESI-MS/MS—V79 Chinese hamster lung fibroblasts (6 million cells, in duplicate) were treated with 100 μM DEB for 3 hours. Following treatment, DEB-containing media was replaced with fresh media, and the cells were allowed to recover for 0.5, 0.75, 1, 2, or 24 hours to allow for adduct repair. To quantify the remaining 1,N^6-HMHP-dA adducts, cells were harvested with 5 mL of PBS, sedimented, and stored at −20 °C until DNA extraction.

DNA extraction from cells was performed using standard phenol-chloroform extraction. DNA concentrations were determined by UV spectrophotometry (Thermo Scientific, Waltham, MA, USA) based on the absorbance at 260 nm. DNA purity was assessed from

A_{260}/A_{280} absorbance ratios, which were typically between 1.8 and 1.9. DNA (50–150 μg) was re-suspended in water (200 μL).

DNA (100 μg) was spiked with $^{15}N_4$-1, N^6-HMHP-dA internal standard (27.5 fmol) and enzymatically digested with DNase I (35 U/100 μg DNA), PDE I (70 mU/100 μg DNA), PDE II (80 mU/100 μg DNA), and alkaline phosphatase (14.6 U/100 μg DNA) in 10 mM Tris-HCl/15 mM $MgCl_2$ at 37 °C for 18 h.[27] 1, N^6-HMHP-dA and its internal standard were isolated by solid phase extraction using Extract Clean Carbo cartridges (3 mL, from Grace Davidson, Deerfield, IL). SPE cartridges were washed with methanol (2 × 3 mL) and water (2 × 3 mL) prior to loading samples in water (1 mL). Samples were washed with water (3 mL) and 5 % methanol (3 mL) and eluted with 30 % methanol (3 mL). The 30 % methanol elution was dried under vacuum and re-dissolved in 25 μL 0.05% acetic acid. Typically, 8 μL of this solution was injected on column for HPLC-ESI^+-MS/MS analysis.

DNA hydrolysates containing *1,*N^6-HMHP-dA were analyzed by column switching HPLC-ESI^+-MS/MS methods as reported elsewhere.[27] In brief, trapping was achieved with a 300 Å SCX column (Waters Corp., Milford, MA) using an isocratic flow of 0.5% methanol in 1mM ammonium hydroxide in water. Samples were then back-flushed with 0.05% acetic acid to transfer *1,*N^6-α-HMHP-dA and its internal standard onto a Synergi Hydro-RP (250 × 0.5 mm, Phenomenex) analytical column. The solvent system consisted of 0.05% (v/v) acetic acid (A) and methanol (B) delivered at a flow rate of 10 μL/min. Solvent composition was changed linearly from 0.5 % to 5% B in 5 min, and further to 20% B in 10 min. The mass spectrometer was operated in the selected reaction monitoring mode by following the neutral loss of deoxyribose from the $[M+H]^+$ ions of *1,*N^6-HMHP-dA and the $^{15}N_4$-internal standard (*m/z* 338.1 → 222.1 and *m/z* 342.1 → 226.1, respectively). Quantitation was performed by comparing HPLC- ESI^+-MS/MS peak areas corresponding to the analyte and its internal standard using standard curves constructed with authentic standards.

Synthesis of site-specifically modified DNA substrates

Synthetic oligodeoxynucleotides containing site- and stereospecific (*S*)-N^6-HB-dA, (*R,S*)-1,N^6-HMHP-dA, and (*R,R*)-N^6,N^6-DHB-dA lesions were prepared by the post-oligomerization methodology developed in our laboratory.[28–30] Briefly, (*R,S*)-1,N^6-HMHP-dA adducted DNA strands were prepared by coupling (*R,R*)-*N*-Fmoc-1-amino-2-hydroxy-3,4-epoxybutane with the oligomers containing site-specific 6-chloropurine at position ***X***. The resulting (*R,R*)-N^6-(2-hydroxy-3,4-epoxybut-1-yl)-adenine (*R,R*-HEB-dA) containing oligodeoxynucleotides were isolated by high performance liquid chromatography (HPLC) and subjected to cyclization in water to afford the corresponding (*R,S*)-1,N^6-HMHP-dA strands. The corresponding oligomers containing (*S*)-N^6-HB-dA and *(R,R)*-N^6,N^6-DHB-dA adducts were prepared via nucleophilic aromatic substitution of 6-chloropurine-containing DNA on solid support with (*S*)-*N*-Fmoc-1-aminobut-3-en-2-ol and (*R,R*)-pyrrolidine-3,4-diol, respectively (Scheme 2).[29] Adduct-containing oligodeoxynucleotides were cleaved off solid support using 0.1 M NaOH for three days at room temperature.[29] DNA strands containing 5-fluoro-dU, 8-oxo-dG and 1,N^6-etheno-dA at position ***X*** (positive controls for BER experiments) were prepared by solid phase synthesis using commercially available phosphoramidites (Glen Research, Sterling, VA). The

modified nucleotides were added using an offline manual coupling protocol. The 8-oxo-dG-containing oligomer was subsequently oxidized with Na_2IrCl_6 to generate the corresponding guanidinohydantoin-containing strands.[31] All DNA strands were purified by reversed phase HPLC and characterized by HPLC-ESI-MS (Table 1), ESI-MS/MS of total enzymatic digests (Figure S-1A–C), and MALDI-TOF-MS of exonuclease ladders (Figure S1 D–E). Synthetic DNA strands were quantified by UV spectrophotometry.[28]

Preparation of 18-mer DNA duplex 3 by ligation

18-mer DNA strands containing site- and stereospecific (*S*)-N^6-HB-dA, (*R,S*)-1, N^6-HMHP-dA and (*R,R*)-N^6,N^6-DHB-dA lesions at position ***X*** (5′-CGG AC***X*** AGA AGT TTC CCC-3′) were synthesized by ligating the corresponding lesion-containing 11-mer fragments (5′-CGG AC***X*** AGA AGT-3′) to the 7-mer 5′-TTCCCCC-3′. The 7-mer oligonucleotides (1 nmol) were 5′-phosphorylated by incubation with T4 PNK and 6 mM ATP at 37 °C for two hours in PNK buffer supplied by the manufacturer (final volume, 100 μL). The solution was subsequently heated at 65 °C for 20 min to inactivate the enzyme. The resulting 5′-phosphorylated 7-mer oligonucleotide was mixed with of 11-mer fragment 5′-CGG AC***X*** AGA AGT-3′ and the 22-mer complementary strand (5′-CCGGGGGAACTTCTTGTCCGTT-3′) (1 nmol each), heated at 90 °C for 5 min, and allowed to cool slowly to room temperature over four hours to obtain double-stranded DNA. Ligation was carried out with T4 DNA ligase in 1X ligase buffer supplied by the manufacturer at 16 °C overnight (12–16 hours). Double-stranded DNA was precipitated with ethanol, followed by 12% denaturing polyacrylamide gel electrophoresis to isolate the 18-mer ligation product. Gel bands corresponding to the 18-mer ligated product were excised from the polyacrylamide gel, crushed in buffer (500 mM ammonium acetate, and 100 μM EDTA, pH 8), and incubated overnight at 4°C in a rotary carousel. The DNA solution was subsequently filtered through 0.22 μm Costar Spin-X centrifuge tube filters (Corning, Corning, NY) and purified by ethanol precipitation.

Preparation of human fibrosarcoma nuclear extract

Nuclear protein extracts were prepared according to the method described by Jessberger and Berg.[32] In brief, human fibrosarcoma cells (HT1080) were grown in Dulbecco's modified Eagle's media supplemented with 9% fetal bovine serum (Life Technologies, Grand Island, NY, USA) in 150 mm tissue culture dishes. Cells were cultured in a humidified atmosphere of 5% carbon dioxide and 95% air at 37 °C. HT1080 cells (30–50 million cells/dish) were collected from 15 confluent 150 mm tissue culture dishes, washed three times with ice-cold phosphate buffered saline, and re-suspended in 2 mL of buffer A (10 mM Tris [pH 7.4] containing 10 mM KCl, 10 mM $MgCl_2$, and 10 mM DTT). Following 15 min incubation on ice, phenylmethylsulfonyl fluoride (PMSF) was added to a final concentration of 1 mM, and the cells were mechanically disrupted by 20 strokes in a Dounce homogenizer (tight pestle). The released nuclei were sedimented and re-suspended in 2 mL buffer B (comprised of buffer A supplemented with 350 mM NaCl, 1mM PMSF, 0.5 μg/mL leupeptin, 1.0 μg/μL aprotinin and 0.7 μg/mL pepstatin) and incubated for 60 min on ice. This material was centrifuged at 70,000 rpm in a Beckman TL-100.3 rotor at 4 °C for 30 min. Following the addition of glycerol and β-mercaptoethanol to the final concentrations of 10 % and 10 mM,

respectively, the extract was stored at −80 °C. The total protein concentration was measured using the Bradford assay (2–2.9 mg/mL).

Preparation of radiolabeled DNA substrates for repair experiments

Single-stranded DNA oligodeoxynucleotides containing site-specific *R,S*-1,N^6-HMHP-dA, *S*-N^6-HB-dA, or *R,R*-1,N^6-DHB-dA (250 pmol) were radiolabeled by incubation with T4 PNK (3 μL) and γ-^{32}P ATP (3 μL) at 37 °C for 60 min in PNK buffer (final volume = 20 μL). The solutions were heated at 65 °C for 10 min to inactivate the enzyme and filtered through Illustra Microspin G25 column (GE Healthcare, Pittsburgh, PA) to remove excess γ-^{32}P ATP. The 5′-^{32}P-labeled oligomers were mixed with 1–1.2 molar equivalents of the complementary strands in an annealing buffer (10 mM Tris [pH 7] containing 50 mM NaCl or 20 mM Tris-HCl [pH 7.6], 10 mM EDTA, and 150 mM NaCl), heated at 90 °C for 10 min, and allowed to cool slowly overnight to obtain double stranded DNA.

Base excision repair assays with human fibrosarcoma nuclear extracts

Radiolabeled DNA duplexes **1–3** containing site-specific BD-dA adducts (50 nM) were dissolved in 10 mM HEPES (pH 7.4) buffer containing 100 mM KCl, 1 mM EDTA, 1 mM EGTA and 0.1 mM DTT. For initial assays examining the concentration dependence for repair, 0–12 μg of nuclear protein extract from human fibrosarcoma HT1080 cells was added (in a total volume of 20 μL), and the mixtures were incubated at 37 °C. The repair reactions were allowed to proceed for 2 h, followed by heating at 95 °C for 5 min to inactivate the enzymes prior to gel electrophoresis analysis.

For gel electrophoresis analyses of repair reactions, 15% or 20 % polyacrylamide gels containing 7 M urea were pre-run at a constant power of 15 W for 30 min in a TBE running buffer (89 mM Tris, 89 mM boric acid, 2 mM EDTA). Formamide denaturing dye (8 μL, containing 80% formamide, 0.025% xylene cyanol, 0.025% bromophenol blue in TBE running buffer) was added to samples prior to loading onto the gel and electrophoresed at a constant power of (15 W) at an ambient temperature. Radiolabeled 18-mer substrates and 11-mer excision products were visualized on the gel using autoradiography by exposure to a storage phosphor screen overnight. Gels were imaged using a Typhoon FLA 7000 imager (GE Healthcare, Pittsburgh, PA). The extent of repair was evaluated by volume analysis using ImageQuant TL 8.0 (GE Healthcare, Pittsburgh, PA). The rate constants for strand cleavage were calculated by fitting the data to a first order rate equation using Origin 9.1 software (OriginLab Corp., Northampton, MA) or GraFit 5.0 software (Erithacus Software Ltd., Horley, Surrey, UK).

To observe time dependent repair, nuclear extracts from HT1080 cells (25 μg) were added to ^{32}P-endlabeled DNA duplexes (50 nM) in a total volume of 50 μL. Aliquots (10 μL) were withdrawn at 0, 15, 30, 75, 120, and 180 min and quenched by the addition of 10 μL of gel loading buffer (20 mM EDTA in 95% formamide containing 0.05% bromophenol blue and 0.05% xylene cyanol), followed by denaturing PAGE analysis as described above.

To establish a role of base excision repair in adduct removal, DNA duplexes were pre-incubated with a known BER inhibitor, methoxyamine (MX, 3 mM) in the reaction buffer at

room temperature for 60 min prior to the addition of nuclear extract, followed by time dependent repair assay as described above.

Base excision repair assay using recombinant enzymes

Strand cleavage assays were performed under single-turnover conditions (STO, [enzyme] > [DNA substrate]). ^{32}P-endlabeled double-stranded DNA substrates (10–50 nM) were incubated with 8–200-fold excess of each recombinant BER enzyme [AAG, Mutyh, two hNEIL1 isoforms (edited and unedited),[33] hOGG1] in a final volume of 20 μL. The recombinant enzymes were purified using previously published protocols.[33–36]

The assay buffer contained 20 mM Tris-HCl (pH 7.6), 10 mM EDTA, 100 μg/mL bovine serum albumin, 30 mM NaCl, while the experiments using hNEIL1 (edited or unedited) included 60 mM NaCl. AAG reaction buffer was 20 mM Tris-HCl buffer (pH 7.8) containing 100 mM KCl, 5 mM β-mercaptoethanol, 2 mM EDTA, 1 mM EGTA, and 50 μg/mL BSA. Reactions were carried out at 37 °C for 60–180 min and quenched by the addition of NaOH to a final concentration of 0.2 M, heated to 90 °C for 5 min to cleave any abasic sites, and then analyzed by denaturing PAGE as described above.

Analysis of cleavage products by liquid chromatography-tandem mass spectrometry

Capillary HPLC-ESI$^-$-MS/MS analyses were performed on an Agilent 1100 capillary HPLC system (Agilent Technologies, Inc., Wilmington, DE) coupled to an Agilent ion trap mass spectrometer (Agilent Technologies, Inc., Wilmington, DE) or a Thermo LTQ Orbitrap Velos mass spectrometer (Thermo Fisher Scientific, Waltham, MA). Liquid chromatography was performed on a Zorbax SB-C18 column (150 mm 0.5 mm, 5 μm, Agilent Technologies, Inc., Santa Clara, CA). The column was eluted at a flow rate of 15 μL/min using a gradient of 15 mM ammonium acetate (A) and acetonitrile (B). The column temperature was maintained at 25 °C. The solvent composition was changed linearly from 0 to 20% B over 20 min, further to 80% B over 2 min, kept at 80% B for another 2 min, and decreased to 0% B within 1 min.

Agilent ion trap mass spectrometer was operated in the ESI$^-$ mode. Target ion abundance value was set to 50,000, and the maximum accumulation time was 300 ms. In a typical experiment, 6–10 average scans were taken in the mass range of *m/z* 200–1600. Nitrogen was used as a nebulizing gas (15 psi) and as a drying gas (5 L/min, 200 °C), while electrospray ionization was achieved at a spray voltage of 3–3.5 kV. A Thermo LTQ Orbitrap Velos mass spectrometer was operated with the following settings: ESI source voltage, 3.5 kV; source current, 6.7 A; auxiliary gas flow rate setting, 0; sweep gas flow rate setting, 0; sheath gas flow setting, 30; capillary temperature, 275 °C; and S-lens RF level, 50%. The MS/MS conditions were as follows: normalized collision energy, 35%; activation Q, 0.25; activation time, 10 ms; product ion scan range, *m/z* 200 – 1600. The identities of the expected excision products (5′-TCAT-3′ and 5′-CGGAC-3′) were confirmed by comparing their experimental MS/MS spectra to their predicted CID fragmentation patterns from Mongo Oligo Mass Calculator version 2.06 (The RNA Institute, College of Arts and Sciences, State University of New York at Albany, http://mods.rna.albany.edu/masspec/Mongo-Oligo).

For mass spectrometry experiments, repair assays were performed with unlabeled DNA duplexes (Scheme 2, 10 μM) in 10 mM HEPES (pH 7.4) buffer containing 100 mM KCl, 1 mM EDTA, 1 mM EGTA and 0.1 mM DTT in a total volume of 20 μL. Following the addition of the nuclear protein extract (5 μg), repair mixtures were incubated at 37 °C for 3 h. Samples were subjected to solid phase extraction using Sep Pak C18 cartridges (100 mg/1 mL) according to the manufacturer suggested protocol (Waters, Milford, MA). SPE fractions containing DNA (70% methanol elution) were dried *in vacuo* and reconstituted in water (20 μL) prior to HPLC-ESI$^-$-MS/MS analysis as described above.

Results

Kinetics of 1,N^6-HMHP-dA adduct removal in mammalian cells

In our initial studies, the repair dynamics of 1,*N*^{6}-HMHP-dA adducts were examined in Chinese hamster lung fibroblasts (V79) treated with 100 μM DEB for 3 hours (Figure 1). Following carcinogen removal, cells were incubated in fresh media for 0.5–24 h to allow for adduct repair. Adduct levels in chromosomal DNA at each post-treatment time point were determined using isotope dilution HPLC-ESI-MS/MS methodology developed in our laboratory.[27] We found that 1,N^6-HMHP-dA adducts were rapidly removed in mammalian cells, with a half life ($t_{1/2}$) of 0.97 h (Figure 1). These results indicate that mammalian cells have an efficient mechanism for removing these types of adducts from genomic DNA.

Synthesis and structural characterization of DNA oligodeoxynucleotides

In order to determine the molecular mechanisms of repair of 1,N^6-HMHP-dA and related BD-dA adducts in human cells, model DNA substrates containing site specific adducts were prepared. Three DNA sequences were selected (Scheme 2). An 11-bp duplex (Duplex **1**) was derived from the human *N-ras* protooncogene, with BD-dA adducts (***X***) inserted at the second position of codon 61: 5′-CGG AC***X*** AGA AG-3′ and 3′-GCC TG***Y*** TCT TC-5′ where ***Y*** = dT or dG.[37] An 18-bp duplex (Duplex **2**, 5′-TCA T***X***G AAT CCT TCC CCC-3′ and 3′-AGT A***Y***C TTA GGA AGG GGG-5′ where ***X*** = BD-dA adduct and ***Y*** = dT or dG) was identical to the sequence used in our published lesion bypass experiments with DNA polymerases.[26] Another 18-bp duplex (Duplex 3, 5′-CGG AC***X*** AGA AGT TTC CCC-3′ and 5′-GGG GAA ACT TCT YGT CCG′3′, where ***X*** = BD-dA adduct and ***Y*** = dT or dG) was prepared by ligating an 11-nt lesion containing strand to a 7 nt strand (5′-TTC CCC-3′) using the 18-nt strand as a template.

A post-oligomerization methodology developed in our laboratory[28,29] was used to generate DNA strands containing (*S*)-*N*^{6}-HB-dA, (*R,R*)-*N*^{6},*N*^{6}-DHB-dA, or (*R,S*)-1,*N*^{6}-γ-HMHP-dA (Scheme 3). In this approach, DNA strands containing 6-chloropurine (***X***) (5′-TCA T***X***G AAT CCT TCC CCC-3′ and 5′-CGG AC***X*** AGA AG-3′) are prepared using solid phase synthesis with commercial 6-chloropurine-2′-deoxyribose phosphoramidite. The resulting 6-chloropurine-containing strands are reacted with (*S*)-N-Fmoc-1-aminobut-3-en-2-ol, (*R,R*)-*N*-Fmoc-1-amino-2-hydroxy-3,4-epoxybutane,[28,29] or commercial (*3R,4R*)-1-benzyl-pyrrolidine-3,4-diol to generate the corresponding oligomers containing site specific (*S*)-*N*^{6}-HB-dA, (*R,R*)-*N*^{6}-(2-hydroxy-3,4-epoxybutan-1-yl)-dA and (*R,R*)-*N*^{6},*N*^{6}-DHB-dA adducts, respectively (Scheme 3).[28,29] DNA strands containing (*R,R*)-*N*^{6}-(2-hydroxy-3,4-

epoxybutan-1-yl)-dA were converted to the corresponding (*R,S*)-1,N^6-HMHP-dA containing strands via intramolecular nucleophilic substitution in an aqueous solution.[28,29] These reactions were conducted on solid support in order to maximize the yield of the final product. All synthetic oligodeoxynucleotides were purified by HPLC to achieve > 98% purity and characterized by liquid chromatography-mass spectrometry (Table 1, Supplement S-1).

Known substrates of mismatch uracil DNA glycosylase (MUG),[38] hNEIL1,[39] hOGG1,[40–42] mouse Mutyh, Nei/Nth,[43,44] and alkyl adenine DNA glycosylase (AAG)[45] [5-fluoro-dU, guanidinohydantoin, 8-oxo-dG:C, 8-oxo-dG:A, thymine glycol, and 1,N^6-etheno-dA (or hypoxanthine), respectively, see Scheme 2] served as positive controls in DNA repair experiments. Synthetic DNA containing 5-fluoro-dU, 8-oxo-dG and 1,N^6-etheno-dA (duplexes **1,** and **2** with adduct at position ***X*,** see Scheme 2) were prepared by solid phase synthesis. 8-oxo-dG was subsequently oxidized to guanidinohydantoin using Na_2IrCl_6.[31] All DNA strands were purified by reversed phase HPLC and characterized by liquid chromatography-mass spectrometry, HPLC-ESI-MS/MS of enzymatic digests, and MALDI-TOF-MS of exonuclease ladders (Table 1, Figure S-1).

Removal of BD-dA adducts using human fibrosarcoma nuclear extract

To observe the efficiency of BD-dA adducts removal in human cells, radiolabeled Duplex **2** containing site- and stereo-specific (*R,S*)-1,N^6-HMHP-dA, (*S*)-N^6-HB-dA, or (*R,R*)-N^6,N^6-DHB-dA at position ***X*** and dT at position ***Y*** (Scheme 2) were incubated with nuclear protein extracts from human fibrosarcoma (HT1080) cells. Repair reactions were resolved on 20% denaturing polyacrylamide gels, and the formation of the 5′-incision product (5′-TCAT-3′) was detected as band that migrated farther in the gel. DNA strands containing all three BD-dA adducts were cleaved by human nuclear extracts in a concentration dependent manner (Figure 2). The kinetics of BD-dA adduct excision by human nuclear proteins was investigated by gel electrophoresis analysis of repair reactions quenched at pre-selected time points (Figure 3A). We found that the excision efficiency was in the order (*S*)-N^6-HB-dA ≈ (*R,R*)-N^6,N^6-DHB-dA > (*R,S*)-1,N^6-HMHP-dA (first order rate constants 0.02, 0.02 and 0.01 min^{-1}, respectively, see Table 2). The extent and the rate of repair decreased significantly in the presence of a known BER inhibitor, methoxyamine (MX)[46] (Figures 3B–D, Table 2).

To compare the efficiency of BD-dA adduct excision by human nuclear protein extracts to that of known BER substrates, the corresponding DNA duplexes containing 5-fluoro-dU (a known MUG substrate),[38] and 8-oxo-dG (a known hOGG1 substrate)[47] were prepared (Positive controls in Scheme 2). Repair reactions with nuclear protein extracts were conducted the same way as for BD-dA adducts. An excision product that migrated with similar mobility was observed for known BER substrates (Figure 4). Furthermore, the efficiency of excision of BD-dA adducts was similar to that of known BER substrates (Figure 4). Based on the experimental first order rate constants (Table 2), all three BD-dA adducts were excised 1.1–1.7-fold faster as compared to 5F-dU, while the rates were 1.3–2.3-fold slower with respect to 8-oxo-dG.

Liquid chromatography-tandem mass spectrometry analysis of base excision repair using nuclear extracts

To confirm that BD-dA lesions are recognized and cleaved via a BER mechanism, cleavage products generated upon incubation of Duplex 2 (Scheme 2, ***X*** = BD-dA adduct and ***Y*** = dT) with nuclear protein extracts from HT1080 cells were analyzed by HPLC-ESI$^-$-MS/MS. Tandem mass spectrometry employing collision-induced dissociation was used to sequence the products. An incision product, 5′-TCAT-3′, was observed for all three adducted DNA duplexes (Figures 5), while negative controls incubated in the absence of nuclear protein extracts were not cleaved (results not shown). This excision product is consistent with a downstream BER intermediate. In this pathway, cleavage of the N-glycosidic bond of a damaged base by a DNA glycosylase generates an apurinic/apyrimidinic (AP) site.[48–50] Further processing of an AP site by an AP endonuclease (APE) results in incision of the DNA strand 5′ to the AP site to generate a single-strand break (SSB) terminating with 3′-hydroxyl.[48–50] Alternatively, the lyase activity of bifunctional glycosylases may cleave DNA from the 3′ side of the AP site to generate a strand break.[48–50] The terminal clean-up step by APE or a 3′-phosphodiesterase would result in formation of a processed 3′-OH-containing DNA fragment, consistent with the observed excision products (Figures 2 and 3).[48–50] Taken together, our HPLC-ESI-MS/MS results corroborate the gel electrophoresis data in Figures 1 and 2, suggesting that all three BD-dA adducts may be processed by a BER mechanism in human cells.

Activity of recombinant BER glycosylases towards BD-dA adducts

In an attempt to identify BER glycosylases that may be involved in the human nuclear protein extract–catalyzed cleavage reactions of BD-dA adducts, radiolabeled duplexes **2** and **3** (Scheme 3) where ***X*** = (*R*,*S*)-1,N^6-HMHP-dA, (*R*,*R*)-N^6,N^6-DHB-dA, and (*S*)-N^6-HB-dA and ***Y*** = dT were incubated with several mammalian glycosylases under single nucleotide turnover conditions. The mammalian glycosylases chosen included human AAG, hNEIL1, hOGG1, and mouse Mutyh. There are two isoforms of hNEIL1 due to RNA editing of its pre-mRNA that differ at amino acid 242 (Lys 242, unedited, and Arg 242, edited) and have been shown to have distinct substrate specificities; therefore, both edited and unedited isoforms were examined in cleavage assays.[33] Repair reactions were quenched by heating in the presence of NaOH to convert any abasic sites formed to DNA strand breaks and resolved on 15% denaturing polyacrylamide gels, where the cleavage products appeared as high mobility bands. DNA duplexes containing known substrates for a given glycosylase were used as positive controls. No cleavage was observed for AAG, hNEIL1 (edited and unedited), and Mutyh (Figure 6). Although certain recombinant glycosylases (most notably, hOGG1) generated some level of strand scission during unusually prolonged incubations (Figure 6), gel mobility of the observed excision products did not match that of authentic standards representing expected cleavage products, suggesting that they formed as a result of a contaminating nuclease. Future studies are needed to identify glycosylase enzymes involved in base excision repair of BD-dA adducts in human cells.

Discussion

Genomic DNA serves as a repository of hereditary information, and its integrity is essential for life.[51–53] However, DNA nucleobases are susceptible to electrophilic attack by chemical and physical agents formed endogenously and present in our diet and the environment. If not repaired, the resulting DNA adducts can lead to mutations and cell death.[51,52,54] Each living cell is equipped with multiple cellular DNA repair mechanisms,[52,55] including direct repair,[52] mismatch repair,[52,56,57] base excision repair (BER),[52,54,56] nucleotide excision repair,[52,56,58,59] homologous recombination,[52,60] and non-homologous end joining.[52,61] Depending on molecular size and shape of specific types of DNA lesions and the extent of helix distortion associated with their formation, they can be removed by one or more mechanism.[52,56]

Our initial experiments conducted in mammalian cell culture (CHO cells, see Figure 1) indicated that 1,N^6-HMHP-dA adducts are rapidly removed by an active repair mechanism ($t_{1/2}$ = 0.97 h). We hypothesized that 1,N^6-HMHP-dA and structurally related N^6-HB-dA and N^6,N^6-DHB-dA adducts are subject to repair by BER because this is the preferred pathway for many relatively small nucleobase lesions that do not drastically disturb DNA structure.[62] For example, structurally related 3-methyladenine and 1,N^6-etheno-dA are recognized and cleaved by alkyladenine DNA glycosylases such as AAG.[63,64] Circular dichroism (CD) experiments indicated that DNA duplexes containing N^6-HB-dA, 1,N^6-HMHP-dA, and N^6,N^6-DHB-dA adducts maintain a B-type DNA conformation.[28] Solution NMR structures of (*R*,*R*) and (*S*,*S*)-N^6,N^6-DHB-dA and (*S*)-N^6-HB-dA containing DNA duplexes show that they are readily accommodated in the major groove of DNA.[65] Only small perturbations in base stacking and hydrogen bonding interactions were observed for (*S*)-N^6-HB-dA, while the presence of N^6,N^6-DHB-dA prevented its hydrogen bonding with thymidine in the opposite strand and disrupted stacking interactions of the adducted base with neighboring nucleotides. The overall B-DNA structure was maintained.[65,66]

Strand incision assays conducted with site-specifically modified DNA duplexes and nuclear extracts from human fibrosarcoma (HT1080) cells (Figures 2,3) suggest that all three BD-dA adducts are efficiently recognized and processed by a BER pathway. In these experiments, 5′-radiolabeled DNA duplexes containing site- and stereospecific BD-dA adducts were incubated with nuclear protein extracts, and the cleavage products were detected as high mobility bands on the gel. Initial cleavage of the modified nucleobase by a BER glycosylase and subsequent excision of the apurinic/apyrimidinic (AP) site by AP endonuclease generates DNA strand breaks. Inhibitor assays repeated in the presence of known BER inhibitor, methoxyamine (MX) showed 50–75 % reduction in repair (Figures 3B–D, Table 2). MX covalently binds to abasic sites generated upon glycosylase-mediated excision of modified nucleobases, preventing their processing by AP endonucleases.[67,68] Kinetic studies have revealed that the efficiency of BER repair of BD-dA adduct was similar to that of known BER substrates such as 8-oxo-dG, 1,N^6-etheno-dA, and 5-fluorouracil (Figure 4). These gel electrophoresis results were confirmed by liquid chromatography-tandem mass spectrometry analyses of the repair reactions, which have detected the expected cleavage products (Figure 5).

Surprisingly, we did not observe significant levels of *in vitro* cleavage of the BD-dA adducts by the four mammalian BER glycosylases tested (mouse Mutyh, human AAG, hOGG1 and hNEIL1, see Figure 6). AAG is known to cleave alkylated adenine lesions such as 3-methyladenine and 1,N^6-ethenoadenine; we initially expected AAG to be a likely candidate in the excision of BD-dA adducts. The mouse Mutyh and human OGG1 glycosylases tested here are best known for their participation in the "GO" repair pathway, which plays an important role in preventing mutations associated with 8-oxo-guanine (OG). The hOGG1 glycosylase removes OG from OG:C bps while Mutyh removes A from OG:A bps that form due to the miscoding propensity of OG.[69,70] We anticipated that Mutyh might be able to removed BD-dA adducts due to the fact that these are derivatives of adenine; however, we did not observe activity *in vitro* for any of the tested glycosylases (Figure 6). These results suggest that other BER enzymes may contribute to repair of these BD-dA adducts in human cells, or that auxiliary factors not included in our *in vitro* experiments are required for efficient excision.[71–73] For example, coordinating action between two or more repair proteins may be required for adduct removal, as previously observed for XRCC1 with PolB or hOGG1.[71,72] and for NEIL1 with the PCNA sliding clamp.[74] The second protein may be required to unwind DNA or to form a scaffold that facilitates the recruitment of BER proteins to lesion site. Alternatively, the exocyclic lesions could be oxidized to secondary adducts by enzymes such as the AlkB proteins, thereby becoming better substrates for known BER glycosylases.[75] Additional studies in repair deficient cells are underway to investigate these possibilities.

Supplementary Material

Refer to Web version on PubMed Central for supplementary material.

Acknowledgments

Funding Source Statement. This research was supported by grants from the National Cancer Institute (CA100670 and CA067985) to NT and SSD, respectively. Douglas Banda was supported by a National Institute of Environmental Health Sciences funded training program in Environmental Health Sciences (T32 ES007059). Amelia Manlove was supported by Grant Number T32-GM008799 from NIGMS-NIH Biotechnology Training Grant. Shaofei Ji is a recipient of the 2015–2016 Excellence Fellowship in Chemistry from the University of Minnesota Department of Chemistry. The contents of this publication are solely the responsibility of the authors and do not necessarily represent the official views of the NIGMS or the NIH.

We thank Robert Carlson (Masonic Cancer Center, University of Minnesota) for preparing figures and schemes for this manuscript.

References

1. Hecht SS. Tobacco smoke carcinogens and lung cancer. J Natl Cancer Inst. 1999; 91:1194–1210. [PubMed: 10413421]
2. White WC. Butadiene production process overview. Chem Biol Interact. 2007; 166:10–14. [PubMed: 17324391]
3. Hoffmann D, Hoffmann I, el Bayoumy K. The less harmful cigarette: a controversial issue a tribute to Ernst L Wynder. Chem Res Toxicol. 2001; 14:767–790. [PubMed: 11453723]
4. Rice JM, Boffetta P. 1,3-Butadiene, isoprene and chloroprene: reviews by the IARC monographs programme, outstanding issues, and research priorities in epidemiology. Chem Biol Interact. 2001; 135–136:11–26.

5. Ward JB Jr, Ammenheuser MM, Bechtold WE, Whorton EB Jr, Legator MS. hprt mutant lymphocyte frequencies in workers at a 1,3-butadiene production plant. Environ Health Perspect. 1994; 102(Suppl 9):79–85.
6. Melnick RL, Huff JE. 1,3-Butadiene induces cancer in experimental animals at all concentrations from 6.25 to 8000 parts per million. IARC Sci Publ. 1993:309–322. [PubMed: 8070878]
7. Owen PE, Glaister JR, Gaunt IF, Pullinger DH. Inhalation toxicity studies with 1,3-butadiene. 3 Two year toxicity/carcinogenicity study in rats. Am Ind Hyg Assoc J. 1987; 48:407–413. [PubMed: 3591659]
8. Sasiadek M, Norppa H, Sorsa M. 1,3-Butadiene and its epoxides induce sister-chromatid exchanges in human lymphocytes *in vitro*. Mutat Res. 1991; 261:117–121. [PubMed: 1922154]
9. Carmical JR, Nechev LV, Harris CM, Harris TM, Lloyd RS. Mutagenic potential of adenine N^6 adducts of monoepoxide and diolepoxide derivatives of butadiene. Environ Mol Mutagen. 2000; 35:48–56. [PubMed: 10692227]
10. Tretyakova N, Sangaiah R, Yen TY, Gold A, Swenberg JA. Adenine adducts with diepoxybutane: isolation and analysis in exposed calf thymus DNA. Chem Res Toxicol. 1997; 10:1171–1179. [PubMed: 9348440]
11. Tretyakova NY, Sangaiah R, Yen TY, Swenberg JA. Synthesis, characterization, and *in vitro* quantitation of N7-guanine adducts of diepoxybutane. Chem Res Toxicol. 1997; 10:779–785. [PubMed: 9250412]
12. Selzer RR, Elfarra AA. *In vitro* reactions of butadiene monoxide with single- and double- stranded DNA: characterization and quantitation of several purine and pyrimidine adducts. Carcinogenesis. 1999; 20:285–292. [PubMed: 10069466]
13. Seneviratne U, Antsypovich S, Goggin M, Dorr DQ, Guza R, Moser A, Thompson C, York DM, Tretyakova N. Exocyclic deoxyadenosine adducts of 1,2,3,4-diepoxybutane: synthesis, structural elucidation, and mechanistic studies. Chem Res Toxicol. 2010; 23:118–133. [PubMed: 19883087]
14. Zhang XY, Elfarra AA. Identification and characterization of a series of nucleoside adducts formed by the reaction of 2′-deoxyguanosine and 1,2,3,4-diepoxybutane under physiological conditions. Chem Res Toxicol. 2003; 16:1606–1615. [PubMed: 14680375]
15. Goggin M, Loeber R, Park S, Walker V, Wickliffe J, Tretyakova N. HPLC-ESI$^+$-MS/MS analysis of *N7*-guanine-*N7*-guanine DNA cross-links in tissues of mice exposed to 1,3-butadiene. Chem Res Toxicol. 2007; 20:839–847. [PubMed: 17455958]
16. Park S, Tretyakova N. Structural characterization of the major DNA- DNA cross-link of 1,2,3,4-diepoxybutane. Chem Res Toxicol. 2004; 17:129–136. [PubMed: 14966999]
17. Park S, Hodge J, Anderson C, Tretyakova NY. Guanine-adenine DNA cross-linking by 1,2,3,4-diepoxybutane: potential basis for biological activity. Chem Res Toxicol. 2004; 17:1638–1651. [PubMed: 15606140]
18. Tretyakova N, Livshits A, Park S, Bisht B, Goggin M. Structural elucidation of a novel DNA-DNA cross-link of 1,2,3,4-diepoxybutane. Chem Res Toxicol. 2007; 20:284–289. [PubMed: 17305410]
19. Michaelson-Richie ED, Loeber RL, Codreanu SG, Ming X, Liebler DC, Campbell C, Tretyakova NY. DNA-protein cross-linking by 1,2,3,4-diepoxybutane. J Proteome Res. 2010; 9:4356–4367. [PubMed: 20666492]
20. Gherezghiher TB, Ming X, Villalta PW, Campbell C, Tretyakova NY. 1,2,3,4-Diepoxybutane-induced DNA–protein cross-linking in human fibrosarcoma (HT1080) cells. J Proteome Res. 2013; 12:2151–2164. [PubMed: 23506368]
21. Boysen G, Pachkowski BF, Nakamura J, Swenberg JA. The formation and biological significance of N7-guanine adducts. Mutat Res. 2009; 678:76–94. [PubMed: 19465146]
22. Recio L, Steen AM, Pluta LJ, Meyer KG, Saranko CJ. Mutational spectrum of 1,3-butadiene and metabolites 1,2-epoxybutene and 1,2,3,4-diepoxybutane to assess mutagenic mechanisms. Chem Biol Interact. 2001; 135–136:325–341.
23. Cochrane JE, Skopek TR. Mutagenicity of butadiene and its epoxide metabolites: II. Mutational spectra of butadiene, 1,2-epoxybutene and diepoxybutane at the *hprt* locus in splenic T cells from exposed B6C3F1 mice. Carcinogenesis. 1994; 15:719–723. [PubMed: 8149486]
24. Steen AM, Meyer KG, Recio L. Characterization of hprt mutations following 1,2-epoxy-3-butene exposure of human TK6 cells. Mutagenesis. 1997; 12:359–364. [PubMed: 9379915]

25. Kotapati S, Wickramaratne S, Esades A, Boldry EJ, Quirk DD, Pence MG, Guengerich FP, Tretyakova NY. Polymerase bypass of N^6-deoxyadenosine adducts derived from epoxide metabolites of 1,3-butadiene. Chem Res Toxicol. 2015; 28:1496–1507. [PubMed: 26098310]
26. Kotapati S, Maddukuri L, Wickramaratne S, Seneviratne U, Goggin M, Pence MG, Villalta P, Guengerich FP, Marnett L, Tretyakova N. Translesion synthesis across 1,N^6-(2-hydroxy-3-hydroxymethylpropan- 1,3-diyl)-2′-deoxyadenosine (1,N^6-γ-HMHP-dA) adducts by human and archebacterial DNA polymerases. J Biol Chem. 2012; 287:38800–38811. [PubMed: 22977231]
27. Goggin M, Seneviratne U, Swenberg JA, Walker VE, Tretyakova N. Column switching HPLC-ESI $^+$-MS/MS methods for quantitative analysis of exocyclic dA adducts in the DNA of laboratory animals exposed to 1,3-butadiene. Chem Res Toxicol. 2010; 23:808–812. [PubMed: 20229982]
28. Seneviratne U, Antsypovich S, Quirk-Dorr D, Dissanayake T, Kotapati S, Tretyakova NY. DNA oligomers containing site-specific and stereospecific exocyclic deoxyadenosine adducts of 1,2,3,4-diepoxybutane: synthesis, characterization, and effects on DNA structure. Chem Res Toxicol. 2010; 23:1556–1567. [PubMed: 20873715]
29. Wickramaratne S, Seiler CL, Tretyakova NY. Synthesis of DNA oligodeoxynucleotides containing site-specific 1,3-butadiene- deoxyadenosine lesions. Curr Protoc Nucleic Acid Chem. 2015; 61:4.
30. Quirk Dorr D, Murphy K, Tretyakova N, Dorr DQ. Synthesis of DNA oligodeoxynucleotides containing structurally defined N^6-(2-hydroxy-3,4-buten-1-yl)-adenine adducts of 3,4-epoxy-1-butene. Chem Biol Interact. 2007; 166:104–111. [PubMed: 16765925]
31. Zhao X, Muller JG, Halasyam M, David SS, Burrows CJ. *In vitro* ligation of oligodeoxynucleotides containing *C8*-oxidized purine lesions using bacteriophage T4 DNA ligase. Biochemistry. 2007; 46:3734–3744. [PubMed: 17323928]
32. Jessberger R, Berg P. Repair of deletions and double-strand gaps by homologous recombination in a mammalian in vitro system. Mol Cell Biol. 1991; 11:445–457. [PubMed: 1986239]
33. Yeo J, Goodman RA, Schirle NT, David SS, Beal PA. RNA editing changes the lesion specificity for the DNA repair enzyme NEIL1. Proc Natl Acad Sci U S A. 2010; 107:20715–20719. [PubMed: 21068368]
34. Engstrom LM, Brinkmeyer MK, Ha Y, Raetz AG, Hedman B, Hodgson KO, Solomon EI, David SS. A zinc linchpin motif in the MUTYH glycosylase interdomain connector is required for efficient repair of DNA damage. J Am Chem Soc. 2014; 136:7829–7832. [PubMed: 24841533]
35. Leipold MD, Workman H, Muller JG, Burrows CJ, David SS. Recognition and removal of oxidized guanines in duplex DNA by the base excision repair enzymes hOGG1, yOGG1, and yOGG2. Biochemistry. 2003; 42:11373–11381. [PubMed: 14503888]
36. Lau AY, Scharer OD, Samson L, Verdine GL, Ellenberger T. Crystal structure of a human alkylbase-DNA repair enzyme complexed to DNA: mechanisms for nucleotide flipping and base excision. Cell. 1998; 95:249–258. [PubMed: 9790531]
37. Xu W, Merritt WK, Nechev LV, Harris TM, Harris CM, Lloyd RS, Stone MP. Structure of the 1,4-bis(2′-deoxyadenosin-N^6-yl)-2S,3S-butanediol intrastrand DNA cross-link arising from butadiene diepoxide in the human *N-ras* codon 61 sequence. Chem Res Toxicol. 2007; 20:187–198. [PubMed: 17256975]
38. Liu P, Burdzy A, Sowers LC. Substrate recognition by a family of uracil-DNA glycosylases: UNG, MUG, and TDG. Chem Res Toxicol. 2002; 15:1001–1009. [PubMed: 12184783]
39. Zhao X, Krishnamurthy N, Burrows CJ, David SS. Mutation versus repair: NEIL1 removal of hydantoin lesions in single-stranded, bulge, bubble, and duplex DNA contexts. Biochemistry. 2010; 49:1658–1666. [PubMed: 20099873]
40. Lu R, Nash HM, Verdine GL. A mammalian DNA repair enzyme that excises oxidatively damaged guanines maps to a locus frequently lost in lung cancer. Curr Biol. 1997; 7:397–407. [PubMed: 9197244]
41. Tchou J, Michaels ML, Miller JH, Grollman AP. Function of the zinc finger in Escherichia coli Fpg protein. J Biol Chem. 1993; 268:26738–26744. [PubMed: 8253809]
42. Tchou J, Grollman AP. The catalytic mechanism of Fpg protein. Evidence for a Schiff base intermediate and amino terminus localization of the catalytic site. J Biol Chem. 1995; 270:11671–11677. [PubMed: 7744806]

43. Harrison L, Hatahet Z, Purmal AA, Wallace SS. Multiply damaged sites in DNA: interactions with Escherichia coli endonucleases III and VIII. Nucleic Acids Res. 1998; 26:932–941. [PubMed: 9461450]
44. Miller H, Fernandes AS, Zaika E, McTigue MM, Torres MC, Wente M, Iden CR, Grollman AP. Stereoselective excision of thymine glycol from oxidatively damaged DNA. Nucleic Acids Res. 2004; 32:338–345. [PubMed: 14726482]
45. Lee CY, Delaney JC, Kartalou M, Lingaraju GM, Maor-Shoshani A, Essigmann JM, Samson LD. Recognition and processing of a new repertoire of DNA substrates by human 3-methyladenine DNA glycosylase (AAG). Biochemistry. 2009; 48:1850–1861. [PubMed: 19219989]
46. Liu L, Gerson SL. Therapeutic impact of methoxyamine: blocking repair of abasic sites in the base excision repair pathway. Curr Opin Investig Drugs. 2004; 5:623–627.
47. Hazra TK, Hill JW, Izumi T, Mitra S. Multiple DNA glycosylases for repair of 8-oxoguanine and their potential *in vivo* functions. Prog Nucleic Acid Res Mol Biol. 2001; 68:193–205. [PubMed: 11554297]
48. Fortini P, Pascucci B, Parlanti E, D'Errico M, Simonelli V, Dogliotti E. The base excision repair: mechanisms and its relevance for cancer susceptibility. Biochimie. 2003; 85:1053–1071. [PubMed: 14726013]
49. Kim YJ, Wilson DM III. Overview of base excision repair biochemistry. Curr Mol Pharmacol. 2012; 5:3–13. [PubMed: 22122461]
50. Memisoglu A, Samson L. Base excision repair in yeast and mammals. Mutat Res. 2000; 451:39–51. [PubMed: 10915864]
51. Clancy S. DNA damage & repair: mechanisms for maintaining DNA integrity. Nat Educ. 2008; 1:103.
52. Geacintov, NE.; Broyde, S. Introduction and Perspectives on the Chemistry and Biology of DNA Damage. In: Geacintov, NE.; Broyde, S., editors. The Chemical Biology of DNA Damage. Wiley; Hoboken, NJ: 2010. p. 3-20.
53. Borges HL, Linden R, Wang JY. DNA damage-induced cell death: lessons from the central nervous system. Cell Res. 2008; 18:17–26. [PubMed: 18087290]
54. Hegde ML, Hazra TK, Mitra S. Early steps in the DNA base excision/single-strand interruption repair pathway in mammalian cells. Cell Res. 2008; 18:27–47. [PubMed: 18166975]
55. Huen MS, Chen J. The DNA damage response pathways: at the crossroad of protein modifications. Cell Res. 2008; 18:8–16. [PubMed: 18087291]
56. Yang W. Structure and mechanism for DNA lesion recognition. Cell Res. 2008; 18:184–197. [PubMed: 18157156]
57. Li GM. Mechanisms and functions of DNA mismatch repair. Cell Res. 2008; 18:85–98. [PubMed: 18157157]
58. Shuck SC, Short EA, Turchi JJ. Eukaryotic nucleotide excision repair: from understanding mechanisms to influencing biology. Cell Res. 2008; 18:64–72. [PubMed: 18166981]
59. Fousteri M, Mullenders LH. Transcription-coupled nucleotide excision repair in mammalian cells: molecular mechanisms and biological effects. Cell Res. 2008; 18:73–84. [PubMed: 18166977]
60. Li X, Heyer WD. Homologous recombination in DNA repair and DNA damage tolerance. Cell Res. 2008; 18:99–113. [PubMed: 18166982]
61. Weterings E, Chen DJ. The endless tale of non-homologous end- joining. Cell Res. 2008; 18:114–124. [PubMed: 18166980]
62. Sancar A. DNA excision repair. Annu Rev Biochem. 1996; 65:43–81. [PubMed: 8811174]
63. Wyatt MD, Allan JM, Lau AY, Ellenberger TE, Samson LD. 3-methyladenine DNA glycosylases: structure, function, and biological importance. Bioessays. 1999; 21:668–676. [PubMed: 10440863]
64. Saparbaev M, Kleibl K, Laval J. *Escherichia coli*, *Saccharomyces cerevisiae*, rat and human 3-methyladenine DNA glycosylases repair 1,N^6-ethenoadenine when present in DNA. Nucleic Acids Res. 1995; 23:3750–3755. [PubMed: 7479006]
65. Kowal EA, Seneviratne U, Wickramaratne S, Doherty KE, Cao X, Tretyakova N, Stone MP. Structures of exocyclic *R,R*- and *S,S*-N^6,N^6-(2,3-dihydroxybutan-1,4-diyl)-2′-deoxyadenosine

adducts induced by 1,2,3,4-diepoxybutane. Chem Res Toxicol. 2014; 27:805–817. [PubMed: 24741991]

66. Kowal EA, Wickramaratne S, Kotapati S, Turo M, Tretyakova N, Stone MP. Major groove orientation of the (2S)-N^6-(2-hydroxy-3-buten-1-yl)-2′-deoxyadenosine DNA adduct induced by 1,2-epoxy-3-butene. Chem Res Toxicol. 2014; 27:1675–1686. [PubMed: 25238403]
67. Liuzzi M, Talpaert-Borle M. A new approach to the study of the base-excision repair pathway using methoxyamine. J Biol Chem. 1985; 260:5252–5258. [PubMed: 2580833]
68. Talpaert-Borle M, Liuzzi M. Reaction of apurinic/apyrimidinic sites with [^{14}C]methoxyamine. A method for the quantitative assay of AP sites in DNA. Biochim Biophys Acta. 1983; 740:410–416. [PubMed: 6349690]
69. David SS, O'Shea VL, Kundu S. Base-excision repair of oxidative DNA damage. Nature. 2007; 447:941–950. [PubMed: 17581577]
70. Oka S, Nakabeppu Y. DNA glycosylase encoded by MUTYH functions as a molecular switch for programmed cell death under oxidative stress to suppress tumorigenesis. Cancer Sci. 2011; 102:677–682. [PubMed: 21235684]
71. Wong HK, Kim D, Hogue BA, McNeill DR, Wilson DM III. DNA damage levels and biochemical repair capacities associated with XRCC1 deficiency. Biochemistry. 2005; 44:14335–14343. [PubMed: 16245950]
72. Wong HK, Wilson DM III. XRCC1 and DNA polymerase beta interaction contributes to cellular alkylating-agent resistance and single-strand break repair. J Cell Biochem. 2005; 95:794–804. [PubMed: 15838887]
73. Dianova II, Sleeth KM, Allinson SL, Parsons JL, Breslin C, Caldecott KW, Dianov GL. XRCC1-DNA polymerase beta interaction is required for efficient base excision repair. Nucleic Acids Res. 2004; 32:2550–2555. [PubMed: 15141024]
74. Dou H, Theriot CA, Das A, Hegde ML, Matsumoto Y, Boldogh I, Hazra TK, Bhakat KK, Mitra S. Interaction of the human DNA glycosylase NEIL1 with proliferating cell nuclear antigen. The potential for replication-associated repair of oxidized bases in mammalian genomes. J Biol Chem. 2008; 283:3130–3140. [PubMed: 18032376]
75. Wauchope OR, Beavers WN, Galligan JJ, Mitchener MM, Kingsley PJ, Marnett LJ. Nuclear oxidation of a major peroxidation DNA adduct, M1dG, in the genome. Chem Res Toxicol. 2015; 28:2334–2342. [PubMed: 26469224]

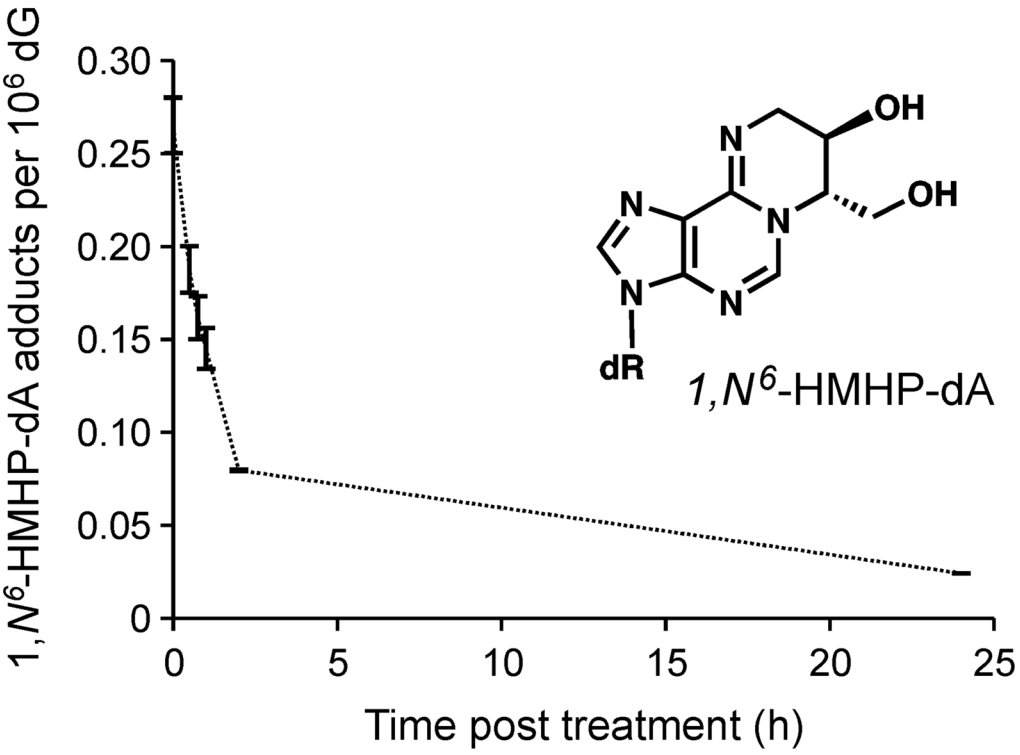

Figure 1.

Dynamics of DEB-induced 1,N^6-HMHP-dA adducts in hamster V79 cells. Cells were treated with 100 μM DEB for 3 hours and allowed to repair the damage for 0.5–24 hours, followed by enzymatic digestion of genomic DNA and HPLC-ESI-MS/MS analysis of any lesions remaining.

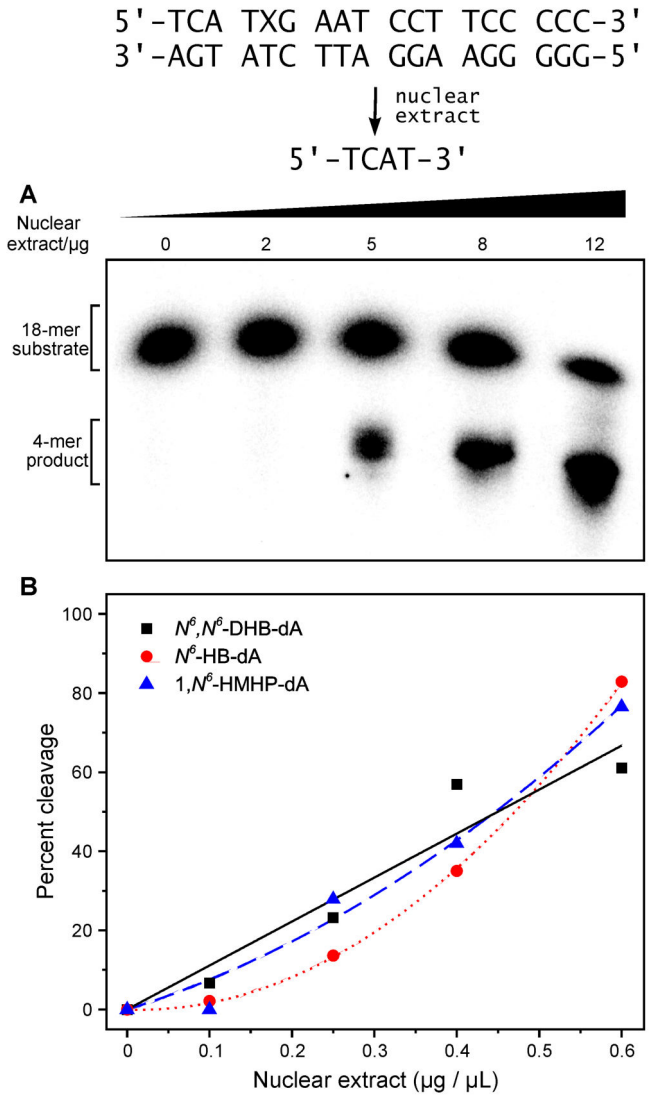

Figure 2.

Concentration dependent cleavage of DNA adducts by nuclear protein extracts from HT1080 cells. ^{32}P-endlabeled DNA 18-mer (5′-TCA T***X***G AAT CCT TCC CCC-3′) duplexes were incubated in 10 mM HEPES (pH 7.4), 100 mM KCl, 1 mM EDTA, 1 mM EGTA and 0.1 mM DTT with increasing amounts of HT1080 nuclear extracts at 37 °C for 2 h. Samples were resolved on a 20% denaturing PAGE gel and visualized by phosphor imaging. (A) A representative PAGE gel for concentration dependent incision of 18-mer containing (*R,S*)-1,N^6-HMHP-dA, and (B) volume analysis showing increasing amounts of incision products for BD-dA adducts with increasing amounts of nuclear extract.

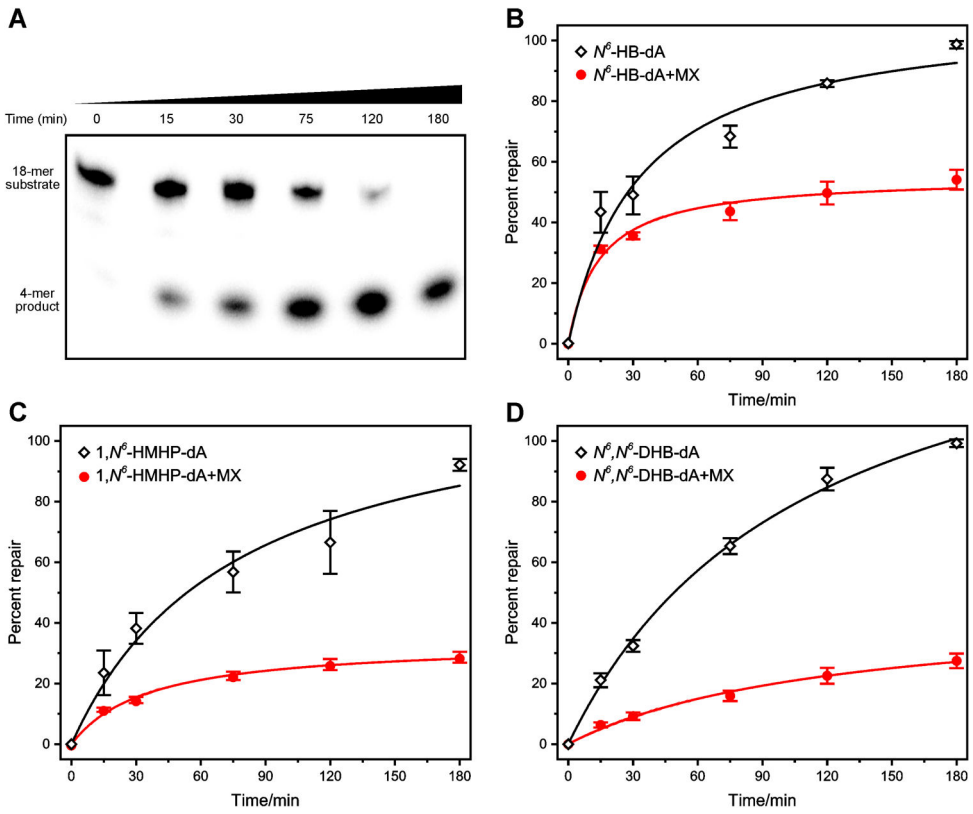

Figure 3.

Time-dependent repair of 1,3-butadiene-induced 2′-deoxyadenosine adducts by nuclear protein extracts from human fibrosarcoma (HT1080) cells. A representative PAGE gel of incision of 18-mer (5′-TCA T***X***G AAT CCT TCC CCC-3′) containing (*R,S*)-1,N^6-HMHP-dA (A), time-dependent incision of 18-mers containing (*S*)-N^6-HB-dA (B), (*R,S*)-1,N^6-HMHP-dA (C), (*R,R*)-N^6,N^6-DHB-dA (D) in the presence (red lines) and absence (black lines) of BER inhibitor, methoxyamine. ^{32}P-endlabeled 18-mer DNA duplexes were incubated with 0.5 μg/μL nuclear extract in 10 mM HEPES (pH 7.4), 100 mM KCl, 1 mM EDTA, 1 mM EGTA and 0.1 mM DTT at 37 °C. Aliquots of the reaction mixture were quenched at preselected time points, samples were resolved on a 20% denaturing PAGE gel and visualized by phosphor imaging. Volume analysis showed increasing amounts of incision products with increasing incubation time (n = 3).

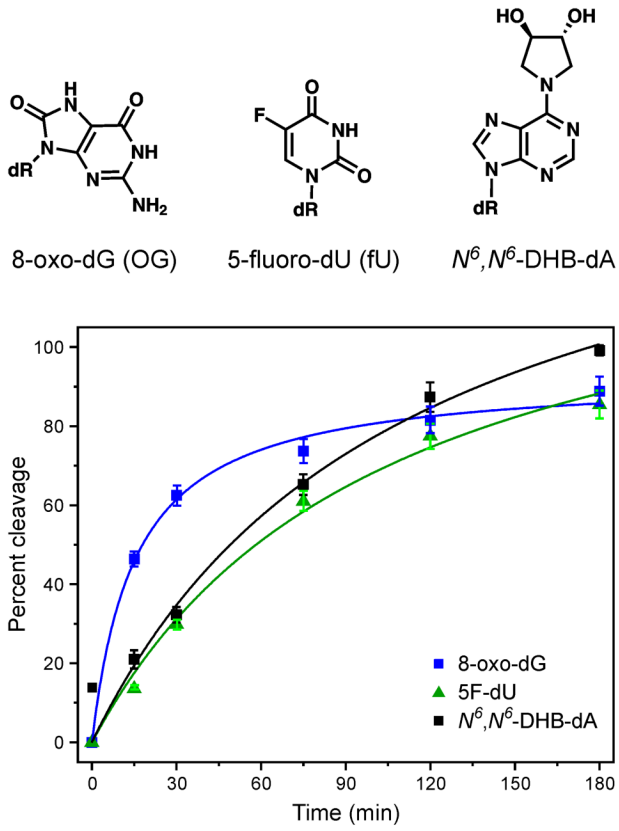

Figure 4.

Time course for excision of N^6,N^6-DHB-dA in the presence of nuclear protein extracts from human cells in comparison to known BER substrates (8-oxo-dG and 5F-dU). ^{32}P-endlabeled dsDNA 18-bp Duplex 2 containing site-specific adducts (50 nM, **X** = N^6,N^6-DHB-dA) was incubated with 0.5 μg/μL nuclear extract in 10 mM HEPES (pH 7.4), 100 mM KCl, 1 mM EDTA, 1 mM EGTA and 0.1 mM DTT at 37 °C. Aliquots of the reaction mixture were quenched at preselected time points, and the samples were resolved on a 20% denaturing PAGE gel and visualized by phosphor-imaging. Volume analysis showed increasing amounts of incision products with increasing incubation time (n = 3).

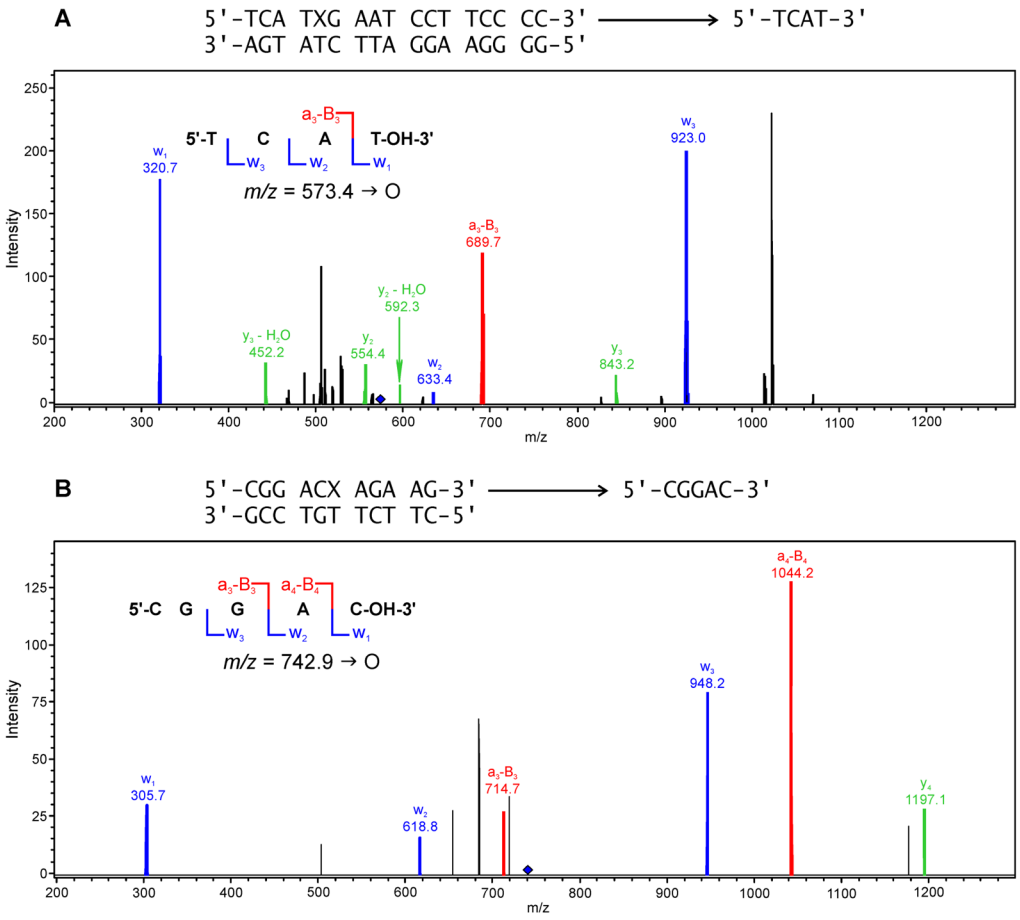

Figure 5.

MS/MS spectra of incision products detected following incubation of DNA duplex 2 containing site specific (*R,S*)-1,N^6-HMHP-dA adducts with nuclear protein extracts from human fibrosarcoma (HT1080) cells.

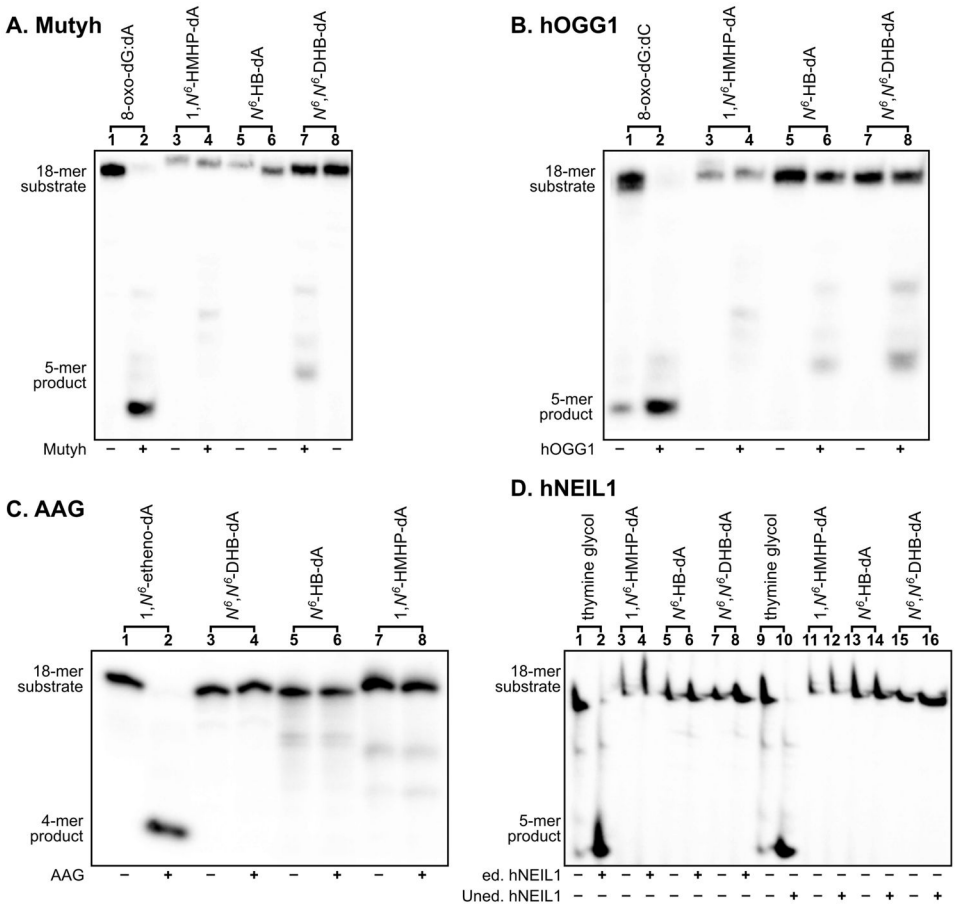

Figure 6.

Base excision repair assay using recombinant mammalian glycosylases: a representative PAGE gel of the repair assay in the presence of (**A**) Mutyh (**B**) hOGG1 (**C**) hAAG, and (**D**) hNEIL1 (edited and unedited) with 18-mer Duplexes 2 (AAG) and Duplex 3 (Mutyh, hOGG1 and hNEIL1) where ***X*** is paired opposite dT. Strand cleavage assays were performed under single-turnover conditions (STO, enzyme concentration > DNA substrate concentration).^{32}P-endlabeled double-stranded DNA substrates (10–50 nM) were incubated with 8–200-fold excess of each recombinant BER enzyme in a final volume of 20 μL. The assay buffer contained 20 mM Tris-HCl (pH 7.6), 10 mM EDTA, 100 μg/mL BSA, 30 mM NaCl, while the experiments using hNEIL1 (edited or unedited) included 60 mM NaCl. AAG reaction buffer was 20 mM Tris-HCl buffer (pH 7.8) containing 100 mM KCl, 5 mM β-mercaptoethanol, 2 mM EDTA, 1 mM EGTA, and 50 μg/mL BSA. Reactions were carried out at 37 °C for 60–180 min and analyzed as described in the methods section.

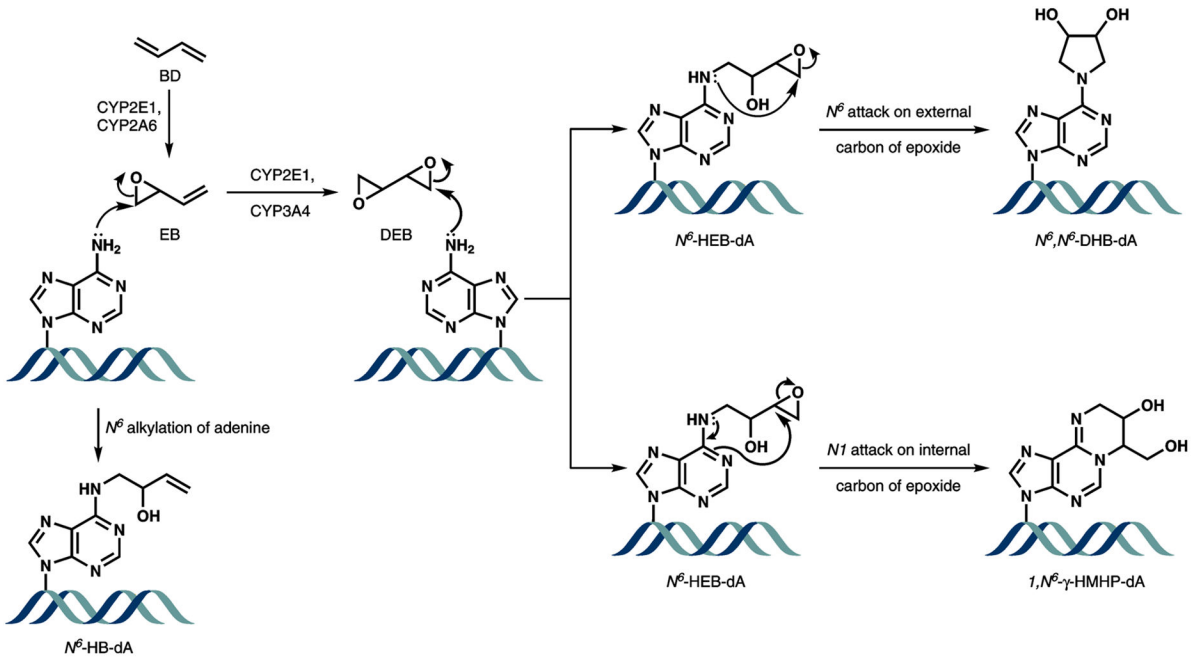

Scheme 1.

Proposed mechanism for the formation of 1,3-butadiene (BD) induced 2′-deoxyadenosine adducts.

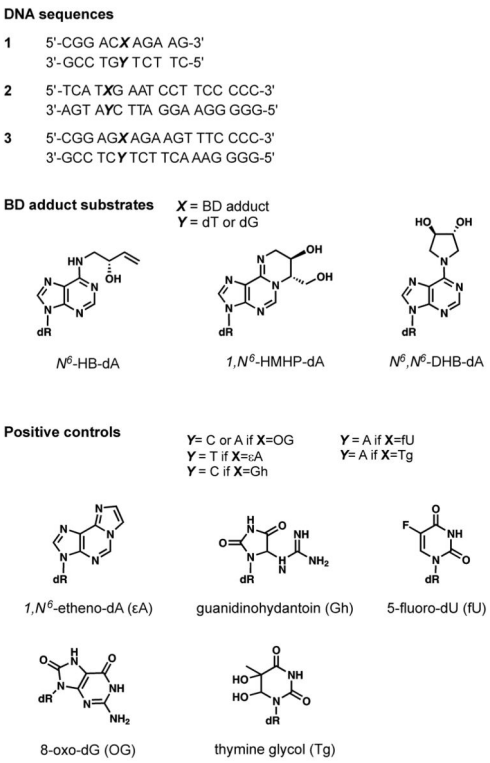

Scheme 2.

DNA sequences and nucleobase lesions employed in the present study.

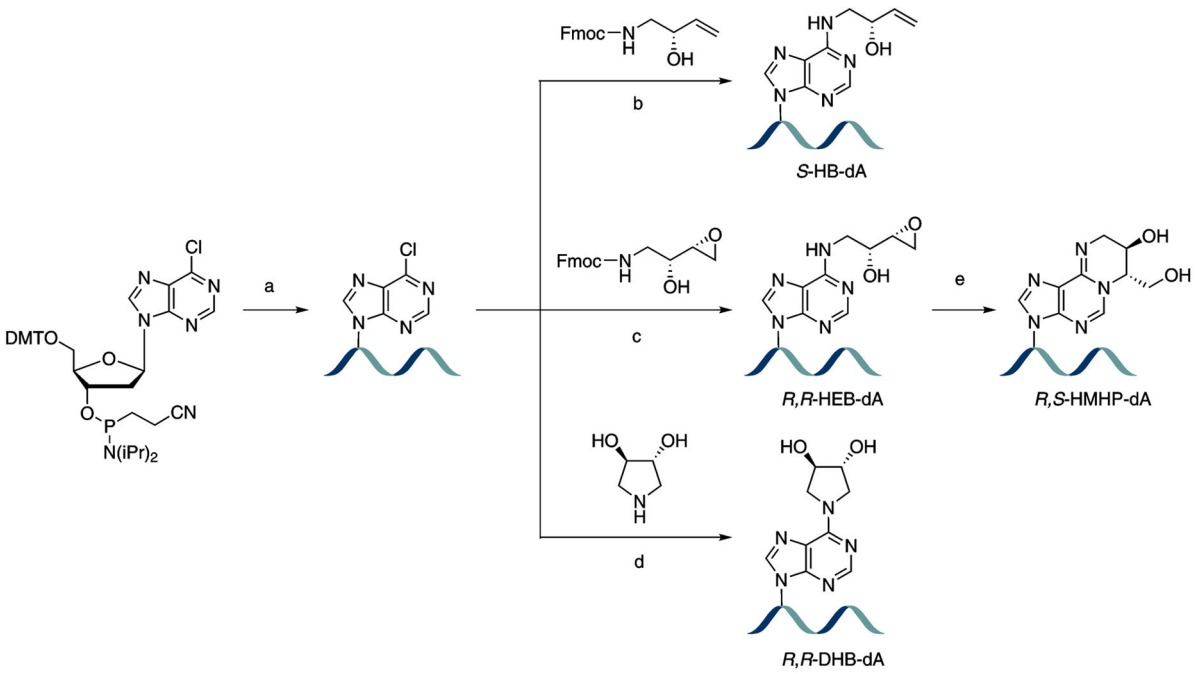

Scheme 3.

Preparation of DNA strands containing site-specific BD-dA adducts by a post-oligomerization approach.

Table 1

HPLC-ESI^{-}-MS characterization of synthetic DNA oligomers.

Oligodeoxynucleotide sequence	Molecular weight/kDa	
	Calculated	Observed
5′-TCA T***X***G AAT CCT TCC CCC-3′; ***X*** = *S*-N^6-HB-dA	5424.5	5424.2
5′-TCA T***X***G AAT CCT TCC CCC-3′; ***X*** = *R*,*S*-1,N^6-HMHP-dA	5440.5	5440.3
5′-TCA T***X***G AAT CCT TCC CCC-3′; ***X*** = *R*,*R*-1,N^6-DHB-dA	5440.5	5440.1
5′-TCA T***X***G AAT CCT TCC CCC-3′; ***X*** = 1,N^6-εdA	5378.5	5378.9
5′-TCA T***Y***G AAT CCT TCC CCC-3′; ***Y*** = 8-oxo-dG	5386.5	5386.1
5′-TCA T***Y***G AAT CCT TCC CCC-3′; ***Y*** = Gh	5376.5	5376.5
5′-TCA T***Z***G AAT CCT TCC CCC-3′; ***Z*** = 5F-dU	5349.4	5349.0
5′-GGG GGA AGG ATT C***T***A TGA-3′	5643.7	5643.4
5′-GGG GGA AGG ATT C***C***A TGA-3′	5628.7	5628.6
5′-GGG GGA AGG ATT C***A***A TGA-3′	5652.8	5652.2
5′-CGG AC***X*** AGA AG-3′; ***X*** = *R*,*S*-1,N^6-HMHP-dA	3485.2	3485.0
5′-CGG AC***X*** AGA AG-3′; ***X*** = *S*-N^6-HB-dA	3469.2	3469.0
5′-CGG AC***X*** AGA AG-3′; ***X*** = *R*,*R*-1,N^6-DHB-dA	3485.2	3484.8
5′-CTT CTT GTC CG-3′	3274.1	3273.8
5′-TCA T-OH-3′	1148.2	1148.2
5′-CGG AC-OH-3′	1487.3	1487.1

Table 2

First order rate constants observed for the repair of BD-dA adducts and known BER substrates by HT1080 nuclear extract.

	DNA adduct	Rate constant ± SE/min^{-1}
HT1080 Nuclear extract	(*S*)-N^6-HB-dA	0.0208 ± 0.0034
	(*S*)-N^6-HB-dA+MX	0.0064 ± 0.0002
	(*R*,*S*)-1,N^6-HMHP-dA	0.0119 ± 0.0013
	(*R*,*S*)-1,N^6-HMHP-dA+MX	0.0024 ± 0.0004
	(*R*,*R*)-N^6,N^6-DHB-dA	0.0152 ± 0.0009
	(*R*,*R*)-N^6,N^6-DHB-dA+MX	0.0020 ± 0.0002
	8-oxo-dG:C	0.0275 ± 0.0061
	5-F-dU:A	0.0119 ± 0.0004